Journal of Photochemistry and Photobiology B: Biology 107 (2012) 73–78

Contents lists available at SciVerse ScienceDirect

Journal of Photochemistry and Photobiology B: Biology

journal homepage: www.elsevier.com/locate/jphotobiol

Differential diagnosis between experimental endophthalmitis and uveitis in vitreous with Raman spectroscopy and principal components analysis

Eglas Emanuel Rossi [a], Antonio Luiz B. Pinheiro [b], Ovidiu C. Baltatu [c], Marcos Tadeu T. Pacheco [c], Landulfo Silveira Jr. [c,*]

[a] Health Sciences Center – CCS, Universidade Comunitária Regional de Chapecó – UNOCHAPECÓ, Chapecó, SC 89809-000, Brazil
[b] School of Dentistry, Universidade Federal da Bahia – UFBA, Salvador, BA 40110-150, Brazil
[c] Biomedical Engineering Center, Universidade Camilo Castelo Branco – UNICASTELO, São José dos Campos, SP 12247-004, Brazil

ARTICLE INFO

Article history:
Received 5 April 2011
Received in revised form 1 December 2011
Accepted 5 December 2011
Available online 13 December 2011

Keywords:
Raman spectroscopy
Vitreous body
Endophthalmitis and uveitis
Differential diagnosis
Discriminant analysis
Principal components analysis

ABSTRACT

Raman spectroscopy has been used for the diagnosis of various eye diseases. A diagnostic tool based on Raman spectroscopy has been developed to discriminate endophthalmitis from uveitis in vitreous tissues of rabbits' eyes *in vitro*. Twenty-two New Zealand rabbits suffering from endophthalmitis induced by *Staphylococcus aureus* ($n = 10$), non-infectious uveitis induced by lipopolysaccharide from *Escherichia coli* (LPS) ($n = 10$ animals) and control ($n = 2$) were included in the study. After eye inoculation, vitreous tissues were dissected and a fragment was submitted to dispersive Raman spectroscopy using near-infrared laser excitation (830 nm, 100 mW) and spectrograph/CCD camera for detection of Raman signal with integration time of 50 s. A routine was developed to classify the spectra of endophthalmitis and uveitis using principal components analysis (PCA) and Mahalanobis distance. The mean Raman spectra of tissues with uveitis and endophthalmitis showed several bands in the region of 800–1800 cm^{-1}, which have been attributed to nucleic acids, amino acids and proteins from inflamed tissue and proliferating bacteria. The bands at 1004, 1258, 1339, 1451 and 1635 cm^{-1} showed statistically significant differences between both diseases. It was observed that principal components PC1, PC3 and PC4 showed statistically significant differences for the two tissue types, indicating that these PCs can be used to discriminate between the two groups. The diagnostic model showed 94% sensitivity, 95% specificity and 95% accuracy using PC3 × PC4. The Raman spectroscopy technique has been shown to be useful in differentiating uveitis and endophthalmitis in vitreous tissues *in vitro*, and these results may be clinically relevant for differentiating vitreous tissues to optimise the diagnosis of inflammatory and infectious vitreoretinal diseases.

1. Introduction

Uveitis and endophthalmitis are both inflammatory processes that affect intraocular tissues. In uveitis, the uveal tractus is completely or partially affected by an inflammation process and it may compromise the other eye tissues such as the retina, optic nerve and vitreous humour [1]. Endophthalmitis consists of an inflammatory process caused by an infectious agent [2–4] and, despite the low incidence of postoperative endophthalmitis (0.04–0.26%), it is one of the most relevant problems in ophthalmology due to its high morbidity and potential hazard of blindness [5].

The differential diagnosis between endophthalmitis and uveitis is difficult, and early diagnosis is important for the success of the treatment [5,6]. These conditions may be treated by sutureless vitrectomy, by a high number of phacoemusification procedures, as well as by intraocular pharmacotherapy, which may increase the risks of endophthalmitis [5]. Moreover, intraocular injection of vascular endothelium growth factor (VEGF) inhibitors or steroids may mask the traditional clinical features of infectious endophthalmitis and it may delay the correct treatment, resulting in bad prognosis for the disease [7].

The diagnosis of uveitis and endophthalmitis is based upon anamnesis, systemic microbiological tests and ophthalmological examinations, which are non-invasive procedures, but diagnostic results are subjective and depend upon the intraocular clinical signals and the expertise of the examiner. Additionally, they may not confirm immediately the aetiological agent [8]. In case of suspicion of infection, the clinician needs to confirm and identify the aetiological agent, and often, this is carried out by using needle aspiration biopsy or pars plana vitrectomy, both with increased risks of damaging the tissues, causing haemorrhage and worsening the infection [8].

* Corresponding author. Address: Universidade Camilo Castelo Branco – UNICASTELO, Núcleo do Parque Tecnológico de São José dos Campos, Rod. Pres. Dutra, km 138, Eugênio de Melo, São José dos Campos, SP 12247-004, Brazil. Tel.: +55 12 3905 4401.
E-mail addresses: landulfo.silveira@unicastelo.br, landulfo.silveira@gmail.com (L. Silveira Jr.).

1011-1344/$ - see front matter © 2011 Elsevier B.V. All rights reserved.
doi:10.1016/j.jphotobiol.2011.12.001

Raman spectroscopy is an optical technique that has been proposed as a discriminating/diagnostic tool in the life sciences [9–14]. This technique is based upon the inelastic scattering interactions between light and matter. These interactions produce spectral bands, formed by photons scattered at the frequencies of the molecular vibrations that provide valuable sensitive and specific information of the biochemical composition of the tissue. This technique has the potential to perform a rapid diagnosis *in vivo*, without trauma (low power excitation source) and without the need for tissue removal or pre-processing, thus, it could become an important tool in ophthalmological diagnosis [15].

Also, Raman technique has been used to monitor the molecular alterations of crystalline lenses with opacities *in situ* [16–18]. Confocal Raman micro-spectroscopy was employed in the evaluation of the composition of vitreous, identifying β-carotene in vitreous asteroid bodies with asteroid hyalosis [19]. Other ophthalmological applications of Raman spectroscopy include the detection of retinal pigments from the macula (lutein and zeaxanthin), the measurement of the level of carotenes in the macula of healthy patients and patients with retinal and choroidal dystrophies, and the quantification of the final products of glycation (AGE) – the proteins modified by non-enzymatic glycation, related to ageing on Bruch's membrane of choroid, the detection and quantification of intraocular drugs, such as ceftazidime and amphotericin B in the aqueous humour of rabbit eyes *in vivo*, and glucose in the anterior chamber of porcine eyes *in vitro* [20–25].

Raman micro-spectroscopy has been used in bacterial identification, to detect and identify different strains of *Staphylococcus* [26,27]. Confocal Raman micro-spectroscopy was used to identify the core and cytoplasm spectra of granulocytes with the aim of diagnosing inflammatory abnormalities [28]. In relation to the leukocyte proliferation and its activation status, the near-infrared Raman spectroscopy was able to detect a reduction in the interleukin-2 production, which was reached by the evaluation of the bands corresponding to the carbon chains [29]. Detecting the infectious agent of the vitreous after its collection with the needle is one of the main challenges of using Raman spectroscopy.

The aims of this study were to identify, through dispersive near-infrared Raman spectroscopy, the spectral differences between vitreous tissues of rabbits suffering from experimentally-induced uveitis (*Escherichia coli* lipopolysaccharides – LPS) and endophthalmitis (*Staphylococcus aureus*), and to develop a discriminating model based on principal components analysis (PCA) and Mahalanobis distance, to be used as a diagnostic tool based upon the spectral characteristics of each condition.

2. Materials and methods

The handling of animals for experimentation followed the guidelines from the Brazilian Committee of Studies in Experimentation Animals (COBEA) and the protocol was approved by the Ethics Committee in Research of the Universidade do Vale do Paraíba. Twenty-two New Zealand albino rabbits weighing 2–3 kg were separated into two groups: G1 – 10 animals with induction of endophthalmitis by intra-vitreous injection of *S. aureus*, and G2 – 10 animals with induction of uveitis through intra-vitreous injection of lipopolysaccharide (LPS) of *E. coli* (LPS, *E. coli* serotype O55:B5 Boivin extract, Sigma–Aldrich, MO, USA). Two animals were used as a control with intra-vitreous injection of 0.1 mL of 0.9% saline.

Prior to the eye injection, rabbits were anaesthetised with intravenous injection of acepram 1.0 mg/kg and diazepam 0.01 mg/kg and immediately after intramuscular injection of 1.0 mL of 1:1 ketamine hydrochloride (100 mg/mL) and xylazine hydrochloride (20 mg/mL) was performed. Pupils were dilated by topical instillation of tropicamide 10% eye drops. Animals from G1 were then submitted to intra-vitreal injection of 0.1 mL solution of 10^5 CFU/mL of *S. aureus*, which was obtained by turbidity of the standard strain [30]. Following this, animals from G2 were submitted to intra-vitreal injection of 500 μg/mL of LPS diluted in 0.1 mL of saline 0.9% [30,31]. The anterior chamber paracentesis (0.1 mL) was carried out before the intravitreal injection with a 27-gauge needle and sterile insulin syringe. These injected suspensions produced clinically observable endophthalmitis and uveitis 24 h after injections. The procedures were performed after conjunctival instillation and washout of topical povidine 5% and povidine 10% was used on the skin following the use of sterile drape.

Twenty-four hours after intra-vitreal injection, the rabbits were euthanised by intracardiac injection of 5.0 mL of thionembutal. In order to confirm the bacterial infection in the G1 and to discard any contamination of G2, an aspiration of the vitreous humour through an insulin needle was carried out in the dead animals and a microorganism culture was performed. Therefore, only positive cultures were included in G1 and negative in G2. The dissection of the vitreous was carried out in a sterile environment, with each vitreous sample placed in a quartz cuvette and the Raman spectroscopy was immediately performed using the Raman spectrometer as shown (Fig. 1), with the technical details described below [32,33]. Raman spectroscopy was performed in both eyes in G1, G2 and control. In addition, the interleukin-1β was measured in all eyes to evaluate the tissue inflammatory response. This experimental protocol was the same as the work of Rossi et al. [33], where the diseased iris tissue was evaluated through Raman technique.

The Raman spectrometer has a diode laser (Micro Laser Systems Inc., CA, USA, model L4830S) with 830 nm wavelength and output power of 80 mW for sample excitation. The cuvette was positioned in 90° excitation–collection geometry, with the scattered light being collected by a set of lenses. The collected light was directed to a laser-rejection notch filter and entered an f/4 imaging spectrograph (Chromex, NM, USA, model 250IS, 600 lines/mm grating) with entrance slit of 200 μm, providing a spectral resolution of about 10 cm^{-1}. The spectrograph was coupled to a liquid-nitrogen cooled CCD camera and a controller (Princeton Instruments, NJ, USA, models LNCCD 1024x256 and ST130, respectively) for the light signal detection. The time exposure to collect each spectrum was set to 50 s. Two spectra were collected for each vitreous sample from G1, G2 and control. Two spectra were also collected from the solution of inoculates (LPS and *S. aureus* in saline).

Spectrograph calibration was checked with naphthalene and all spectra were pre-processed (background fluorescence filtering by a 5th order polynomial fitting and cosmic ray removal manually) using Matlab software (The Mathworks, MA, USA, version 4.2). Each spectrum was normalised by the root-mean-square (RMS) value calculated in the full spectral range (fingerprint region:

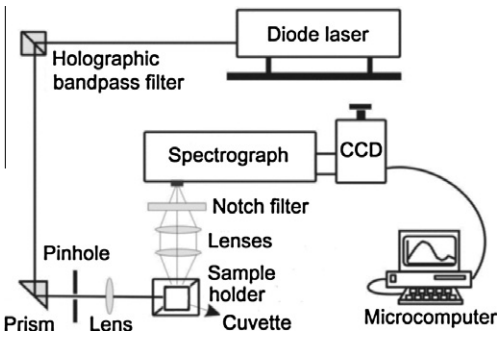

Fig. 1. Schematic diagram of the dispersive Raman spectrometer used in the experiment. Laser power: 80 mW, wavelength: 830 nm, resolution: 10 cm^{-1}. For Raman collection, vitreous body was placed inside a quartz cuvette.

800–1800 cm^{-1}) and mean-centred. For spectral comparison and features identification, the mean spectrum of each lesion group was obtained, and the means of the normal vitreous and of those from the G1 and G2 were plotted.

A classification model was implemented for differential diagnostics of vitreous endophthalmitis and uveitis based on the Raman bands, separating the lesion types according to the differences found in the spectra. For this purpose, the PCA technique was employed to reduce the number of spectral variables and to concentrate the spectral variations in the first principal components. Then, a discriminant analysis based on Mahalanobis distance was applied to correlate the differences in the spectral information of the relevant principal components scores to the lesion type. Herewith, by using PCA, the large dataset can be reduced to a small amount of variables with similar variations, and a discriminant analysis can be employed to determine which spectral characteristics are more correlated with the tissues [32].

Spectra were submitted to the PCA using the ProRaman routine under Matlab [34]. The principal components vectors (containing the spectra of the variances presented in the data) and scores (intensity of each vector in each original spectrum) were obtained from the data set, and these parameters were analysed, seeking a better discrimination. In order to verify which of these vectors best represents the largest differences in the spectral information of vitreous in G1 and G2, and to propose a spectral classification methodology, the Student's *t* test with 5% significance level was applied on the scores of the first four principal components of the two disease groups. Then a discriminant analysis based on the Mahalanobis distance between the endophthalmitis and uveitis was performed to the scatter plot of the principal components scores (PCs). This discrimination is indicated by a diagnostic line based on the mean Mahalanobis distance between the groups. Sensitivity, specificity and accuracy were calculated for the endophthalmitis in relation to the uveitis.

3. Results

All eyes from G1 (endophthalmitis) had a positive culture for *S. aureus* and were used in the spectral analysis. Also, all eyes from G2 (uveitis) had negative culture and were also included in the dataset. The Raman spectra of the solutions of *S. aureus* (10^5 CFU/mL) and LPS (500 μg/mL) did not show visible bands in the fingerprint region, and therefore were not included in the spectral analysis. The spectrum of normal vitreous was presented for band assignment and for comparison with damaged tissues; therefore, it was not used in the statistical analysis.

The mean Raman spectra of vitreous with endophthalmitis infection (G1), non-infection uveitis (G2) and control are shown in Fig. 2.

In the normal vitreous, the Raman spectrum presented a few observable bands around 840 and 1060 cm^{-1}, which could be attributed to the band from hyaluronic acid [35] and Raman scattering of quartz from cuvette [36,37], respectively, and a very low signal-to-noise ratio band at around 1450 cm^{-1}, which could be attributed to CH_2 bending of collagen and hyaluronic acid [10,14,32,38] from the vitreous body. Spectra of non-infection uveitis presented bands at 837 cm^{-1} (overlap of the quartz band and the 850 cm^{-1} band from tyrosine); 1064 cm^{-1} (quartz); 1258 cm^{-1} (amide III: C–H and N–H stretch); 1339 cm^{-1} (amine III: α-helix structure; adenine and guanine; C–H bonds); 1451 cm^{-1} (CH_2 bending of proteins: albumin, lysozyme, ribonuclease; also C–H bonds, including CH_2 and CH_3 from lipids); and 1635 cm^{-1} (1060 cm^{-1} from quartz and a contribution of the 1668 cm^{-1} from amide I vibration: C–C stretching of proteins and lipids in lesser extent) [10,14,16,28,32,38]. Raman spectra of endophthalmitis showed several bands in the same positions of

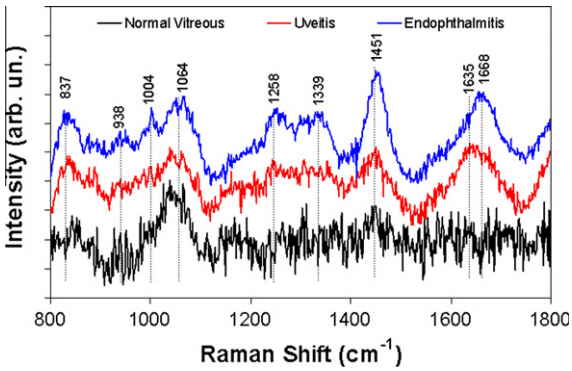

Fig. 2. Mean Raman spectra of vitreous tissues: normal, induced endophthalmitis and induced uveitis. Laser power: 80 mW; wavelength: 830 nm; resolution: 10 cm^{-1}, exposure time: 50 s. The main spectral features of tissues' Raman spectra are indicated with dashed lines. Normal spectrum is shown for Raman features comparison.

uveitis, with a statistically significant increase in the intensity of the bands at 1258, 1339 and 1451 cm^{-1} (*t* test, $p < 0.05$) and a broad band with lower intensity at 938 cm^{-1} (amide III: C–C stretch). Also, a shift of the broad band at 1668 cm^{-1} and a new band at 1004 cm^{-1} (phenylalanine ring from proteins) was observed [10,16,28,38]. Spectral features appearing in endophthalmitis are comparable to those of the staphylococcus [26], mainly the phenylalanine band at 1004 cm^{-1}, bands in the amide III (1250–1350 cm^{-1}) and the very intense CH_2 band at 1451 cm^{-1}. Those bands are in accordance with the basic constitution of bacteria substructural composition, basically nucleic acids (DNA/RNA), proteins, lipids and polysaccharides [26].

Fig. 3 shows the interleukin-1β (IL-1β) values for all groups. This cytokine is involved in a variety of cellular activities, including cell proliferation, differentiation, and apoptosis, and is an important mediator of the inflammatory response. It was found that IL-1β values were increased for the endophthalmitis and uveitis, with higher values for the endophthalmitis, indicating a higher inflammatory response in tissues affected by this infectious process.

A model to classify the Raman spectra of inflamed tissues according to the aetiological agent was developed based on the PCA scores by using the data set of endophthalmitis and uveitis. After extracting the PCA vectors and scores, it was verified that the first four PCs represent about 60% of all spectral variance of the data set (PC1 = 43%, PC2 = 8.0%, PC3 = 3.8%, PC4 = 3.5%). The scores (intensities) of each principal component projected in each one of the Raman spectra (which was related to the relative amount of each PC vector in each spectrum) were used as a differentiation parameter between the lesions, with the use of the Mahalanobis distance as a classification between groups. In order to determine which PC had the most important information to

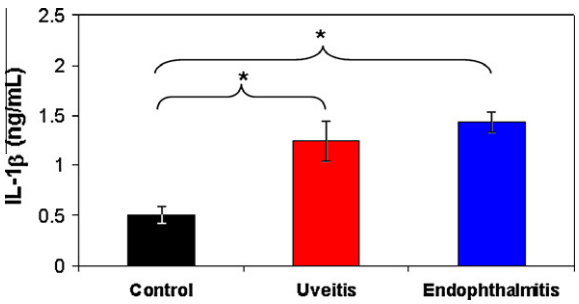

Fig. 3. Interleukin-1β values measured at rabbit eye iris tissues of all groups and control (saline). *Indicated statistically significant differences for control versus uveitis and control versus endophthalmitis (parametric *t*-test, $p < 0.05$).

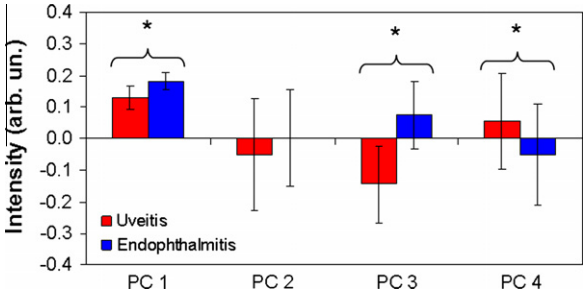

Fig. 4. Mean intensity and standard deviation of the scores of the principal components PC1 to PC4 of the vitreous with endophthalmitis and uveitis. *Indicated statistically significant differences (parametric *t*-test, $p < 0.05$).

describe the spectral variations among the two groups, the mean and standard deviation of the first four PC scores of each lesion group was calculated, and the *t* test with 5% significance level was applied in these scores. Mean values and the standard deviation for the PC1 to PC4 are shown in Fig. 4. It has been verified that the PC1, PC3 and PC4 scores showed statistically significant differences for discriminating G2 from G1.

The spectral vectors from the first four PC vectors of the Raman spectroscopy from G1 and G2 are shown in Fig. 5. It was observed that the principal components PC1 to PC4 resemble Raman spectra with spectral information in the same bands of the endophthalmitis and uveitis tissues. However, the PC3 spectrum presents bands referred to the endophthalmitis spectrum at 1258, 1339 and 1451 cm^{-1}, attributed to the vibrations of C–H and N–H stretch of amide III; α-helix structure and C–H bonds of amine III; CH_2 bending of proteins; and C–H bonds of lipids, including CH_2 and CH_3, respectively. PC4 presents a band at 1668 cm^{-1}, from amide I vibration of proteins and lipids. The presence of higher intensity bands of proteins and lipids in endophthalmitis indicate an inflammatory process taking place, with the spectral contribution arising from proliferating bacteria and inflammatory cells.

The PC1, PC3 and PC4 scores were those that better showed discrimination between the G1 and G2 groups, and they were used in the discrimination model. Fig. 6 shows the scatter plot of PC1 × PC3 and PC3 × PC4 scores, with the Mahalanobis distance being used as a discriminator between the two groups (the mean Mahalanobis distance is also plotted in Fig. 6). Fig. 7 shows the 3-D scatter plot of PC1 × PC3 × PC4 scores.

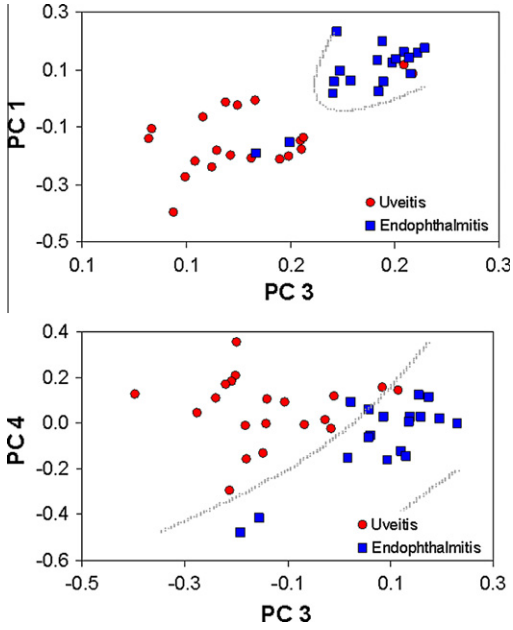

Fig. 6. Scatter plot of the PC3 × PC1 and PC3 × PC4 scores for the vitreous tissues with endophthalmitis and uveitis. Separation lines are based on the mean Mahalanobis distances among groups.

Table 1 shows the results of the spectral classification model of the lesions as well as the sensitivity, specificity and accuracy of the model, with the uveitis being considered as a "benign status" while endophthalmitis was considered a "pathological status". The model indicated maximum sensitivity, specificity and accuracy for the combination of PC3 × PC4.

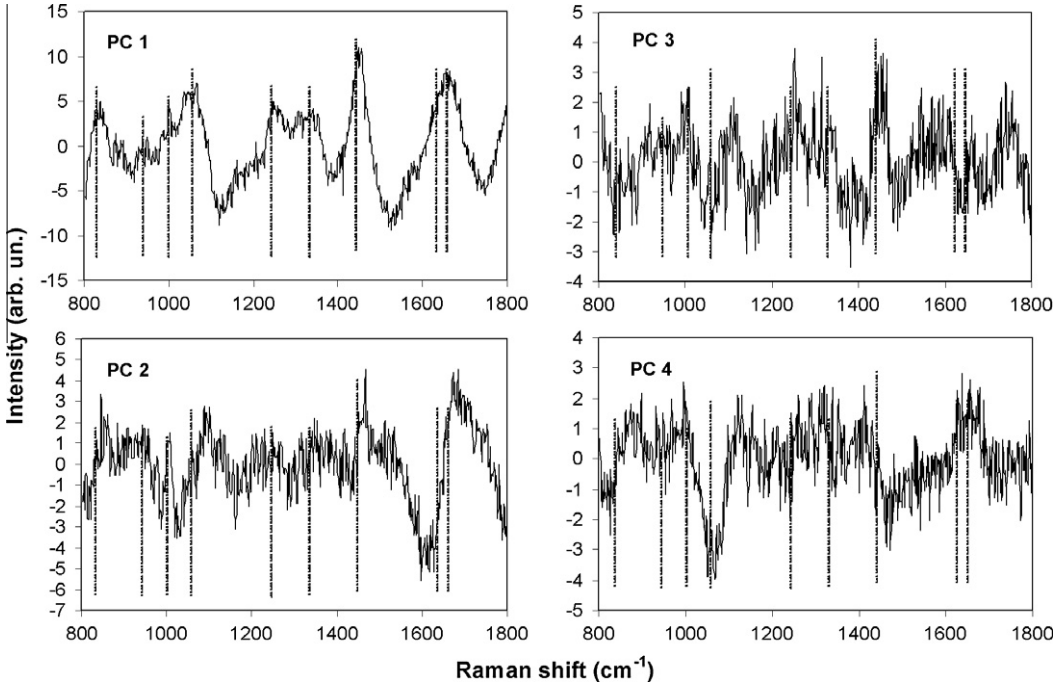

Fig. 5. Plot of the principal components vectors PC1–PC4 for the vitreous tissues, with the main spectral features of Raman spectra indicated with grey dashed lines.

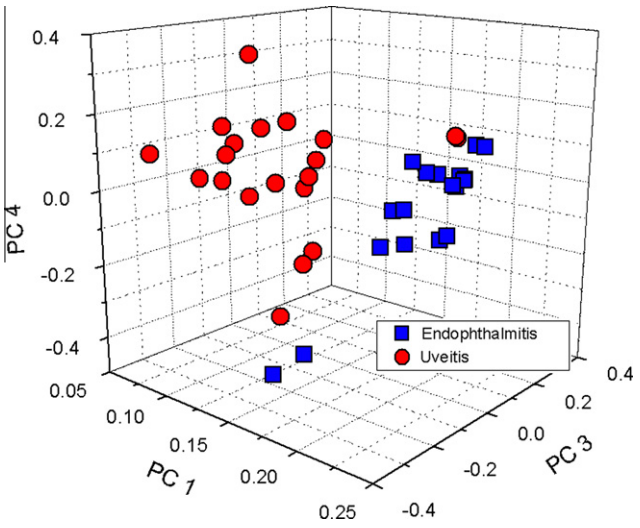

Fig. 7. 3-D scatter plot of the PC1 × PC3 × PC4 scores for the vitreous tissues with endophthalmitis and uveitis.

4. Discussion

Several studies have proposed the use of Raman spectroscopy as a tool for detecting proteins in contact lenses, protein abnormalities in the crystalline lens, vitreous abnormalities and drugs detection in the aqueous humour [15,24,39], aiming for a rapid and minimally invasive diagnostic method in ophthalmology. Due to the molecular specificity, Raman spectra would be able to furnish important and useful biochemical information for diagnosis, helping in the identification of tissue biochemistry and the disease's aetiological agents [10,32].

The normal vitreous is an amorphous hydrogel composed mainly by hyaluronic acid and collagen fibrils immersed in electrolyte solution, mainly NaCl. In this work the vitreous tissue presented a few distinguishable Raman bands in the region between 800 and 1800 cm^{-1}, around 840 and 1060 cm^{-1}, attributed to the hyaluronic acid and quartz cuvette, respectively [35–37]. A very weak band is shown at 1451 cm^{-1} attributed to collagen and hyaluronic acid, demonstrating the feasibility of the detection of proteins in the vitreous tissue [39] through this technique. Raman bands of the vitreous tissue with uveitis (G2) showed weak bands at 1258, 1339 and 1451 cm^{-1} and a relatively strong broad at 1635 cm^{-1}, indicative of the presence of proteins, mainly cytokines, beside leukocytes in the acute phase of the inflammatory process and the nucleic acids of neutrophils, whose concentration is increased in inflamed eye tissues [28].

Analysis of the Raman spectra of vitreous with endophthalmitis (G1) demonstrated an increase in the intensity of the bands at 1258, 1339, 1451 and 1668 cm^{-1} in relation to what is shown in the uveitis and normal vitreous. This is explained by the fact that these bands, related to proteins, lipids and polysaccharides [26], are present in cytokines, leukocytes and also in the *S. aureus* [27], justifying its presence in the infectious process. The new bands at 938 and 1004 cm^{-1} could be attributed to the higher amount of adenine and phenylalanine (ring breathing) from *S. aureus* in the infected tissues, indicating the capability of Raman spectra to recognise spectral features of the *S. aureus* in colonies [26,27,40].

In the experimental uveitis induced by intraocular LPS, it is known that the intensity of the intraocular inflammation presents a maximum response between 20 and 22 h after inoculation; there is also an increase in the vascular permeability and albumin both in tissues and intraocular media, together with an increase in leucocytes, directly related to the amount of LPS injected into the eye [41]. Additionally, in intraocular inflammatory process, there is an increase of cytokines, such as interleukin-6, interleukin-8, tumoural necrosis factor, interleukin-13, γ-interferon and CCL2 [42]. In this study the IL-1β was found to be increased in inflammatory and infected tissues, but the bands related to these cytokines were not found in the literature for a good spectral correlation. It is known that some monoclonal antibodies exhibit a band at around 1245 cm^{-1} [41], which was not observed in this study.

Here, we have shown that it is possible to classify the vitreous spectra depending upon the aetiological agent of the induced lesions (infection/inflammation) by a diagnostic model based on the PCA scores of Raman spectra. The PCA shows the advantage of no need for a previous knowledge of the biochemistry of the tissue under analysis, with just the differences in the spectra from the different samples being important [37,41]. This represents advantages in the development of classification models, considering that it is necessary to know only that there is alteration of the sample, not the nature of this alteration. This is based on the fact that the PCA decomposes the spectra into a new set of variables, the principal components vectors, which represent the directions of the highest spectral variations among all data sets [32,37]. The projection of each observation (spectral data) in each vector comes with new variables, whereas the scores represent the intensity of each PC vector in each tissue spectrum [14].

In the present study, despite the lower signal-to-noise ratio presented by the Raman spectra, the discriminant analysis using the Mahalanobis distance applied to PC3 and PC4 scores showed sensitivity of 94%, specificity of 95% and accuracy of 95%, for the differential diagnosis between endophthalmitis and uveitis. This high sensitivity and specificity from the Raman spectroscopy analysis of infected and inflamed vitreous demonstrates the potential of the Raman spectroscopy for helping the diagnosis of both intraocular pathologies. This is clinically relevant and especially important for differential diagnosis between uveitis and endophthalmitis in eyes with ocular inflammatory response at the postoperative period or after intraocular injection of steroids or inhibitors of VEGF. In these situations, the traditional clinical features of infectious endophthalmitis may be masked and the delay regarding the correct diagnosis

Table 1
Results of the PCA/Mahalanobis diagnostic model applied to Raman spectra of endophthalmitis and uveitis in rabbit's vitreous, with sensitivity, specificity and accuracy values.

	Classification based on the PCA scores and Mahalanobis distance					
	PC1 × PC3		PC3 × PC4		PC1 × PC3 × PC4	
Induced Lesion	Uveitis	Endophthalmitis	Uveitis	Endophthalmitis	Uveitis	Endophthalmitis
Uveitis (n = 20 spectra)	18	2	19	1	18	2
Endophthalmitis (n = 18 spectra)	2	16	1	17	1	17
Sensitivity (%)	89		94		94	
Specificity (%)	90		95		90	
Accuracy (%)	89		95		92	

Note: Sensitivity and specificity calculations were made according to IATROS (Statistics and Scientific Research for Health Care Professionals) and uveitis was considered as a benign disease.

and treatment may result in bad prognosis in cases of infectious endophthalmitis [7].

Raman spectroscopy has become a tool with high potential for the characterisation of biological tissues and the detection of ocular histopathological abnormalities by using the scattering properties of the ocular media [28]. The Raman technique is a potential method to diagnose endophthalmitis from a small vitreous sample obtained during anterior vitrectomy or vitreous biopsy, and prior antibiotics injection through needle. The ability of obtaining quantitative information about the biochemical abnormalities of tissues using dispersive Raman technique and also the possible access to the ocular tissues by this non-destructive technique may become the "optical biopsy" technique, a useful tool for diagnosis of inflammatory and infectious vitreoretinal diseases in clinical ophthalmology.

In order to be able to use the Raman spectroscopy to measure vitreous tissues *in vivo* in a minimally invasive diagnosis, studies to address the problem of light passing through other eye tissues such as the eye lens, which would generate undesired Raman signal, and the safety of the laser power and wavelength to other eye structures such as retina and macula are needed.

Acknowledgements

L. Silveira Jr. thanks CNPq (National Counsel of Technological and Scientific Development) for the Productivity Fellowship (305610/2008-2). Authors thank Prof. Dr. S.R. Zamuner for preparing the *S. aureus* samples and Prof. Dr. F. Aimbire for the interleukin measurements.

References

[1] R.N. Van Gelder, A. Prasad, Review of Uveitis, SLACK Inc., New Jersey, 2008.
[2] M. Taban, A. Behrens, R.L. Newcomb, Acute endophthalmitis following cataract surgery: a systematic review of the literature, Arch. Ophthalmol. 123 (2005) 613–620.
[3] E. Mayer, D. Cadman, P. Ewings, A 10 year retrospective survey of cataract surgery and endophthalmitis in a single eye unit: injectable lenses lower the incidence of endophthalmitis, Br. J. Ophthalmol. 87 (2003) 867–869.
[4] J.J. Miller, I.U. Scott, H.W. Flynn, Acute-onset endophthalmitis after cataract surgery (2000–2004): incidence, clinical settings, and visual acuity outcomes after treatment, Am. J. Ophthalmol. 139 (2005) 983–987.
[5] Endophthalmitis Vitrectomy Study Group, Results of the Endophthalmitis Vitrectomy Study; a randomized trial of immediate vitrectomy and of intravenous antibiotics for the treatment of postoperative bacterial endophthalmitis, Arch. Ophthalmol. 113 (1998) 1479–1496.
[6] A. Turno-Krecicka, M. Misiuk-Hojlo, A. Grzybowski, J. Oficjalska-Mlynczak, M. Jakubowska-Kopacz, J. Jurowska-Liput, Early vitrectomy and diagnostic testing in severe infectious posterior uveitis and endophthalmitis, Med. Sci. Monit. 16 (2010) CR296–CR300.
[7] M. Maia, M.E. Farah, R.N. Belfort, F.M. Penha, A.A. Lima Filho, F.B. Aggio, R. Belfort, Effects of intravitreal triamcinolone acetonide injection with and without preservative, Br. J. Ophthalmol. 91 (2007) 1122–1124.
[8] S.M. Kresloff, A.A. Castellarin, M.A. Zarbin, Management of endophthalmitis, Surv. Ophthalmol. 43 (1998) 193–224.
[9] C.H. Liu, B.B. Das, W.L. Sha Glassman, G.C. Tang, K.M. Yoo, H.R. Zhu, D.L. Akins, S.S. Lubicz, J. Cleary, R. Prudente, E. Celmer, A. Caron, R.R. Alfano, Raman, fluorescence, and time-resolved light scattering as optical diagnostic techniques to separate diseased and normal biomedical media, J. Photochem. Photobiol. B 16 (1992) 187–209.
[10] E.B. Hanlon, R. Manoharan, T.W. Koo, K.E. Shafer, J.T. Motz, M. Fitzmaurice, J.R. Kramer, I. Itzkan, R.R. Dasari, M.S. Feld, Prospects for in vivo Raman spectroscopy, Phys. Med. Biol. 45 (2000) R1–R59.
[11] C.A. Lieber, S.K. Majumder, D.L. Ellis, D.D. Billheimer, A. Mahadevan-Jansen, In vivo nonmelanoma skin cancer diagnosis using Raman microspectroscopy, Lasers Surg. Med. 40 (2008) 461–467.
[12] M.C.M. Grimbergen, C.F.P. van Swol, R.J.A. van Moorselaar, J. Uff, A. Mahadevan-Jansen, N. Stone, Raman spectroscopy of bladder tissue in the presence of 5-aminolevulinic acid, J. Photochem. Photobiol. B 95 (2009) 170–176.
[13] C.B. Lopes, M.T.T. Pacheco, L. Silveira Jr., J. Duarte, M.C.T. Cangussú, A.L.B. Pinheiro, The effect of the association of NIR laser therapy BMPs, and guided bone regeneration on tibial fractures treated with wire osteosynthesis: Raman spectroscopy study, J. Photochem. Photobiol. B 89 (2007) 125–130.
[14] G.V. Nogueira, L. Silveira, A.A. Martin, R.A. Zângaro, M.T. Pacheco, M.C. Chavantes, C.A. Pasqualucci, Raman spectroscopy study of atherosclerosis in human carotid artery, J. Biomed. Opt. 10 (2005) 031117.
[15] N.T. Yu, E. East, Laser Raman spectroscopic studies of ocular lens and its isolated protein fractions, J. Biol. Chem. 6 (1975) 2196–2202.
[16] A. Mizumo, H. Nishigori, M. Iwatsuru, Glucocorticoid-induced cataract in chick embryo monitored by Raman spectroscopy, Invest. Ophthalmol. Vis. Sci. 30 (1989) 132–137.
[17] J.J. Duindam, G.F.M. Vrensen, J. Greve, Cholesterol, phospholipid, and protein changes in focal opacities in the human eye lens, Invest. Ophthalmol. Vis. Sci. 39 (1998) 94–103.
[18] J. Sebag, Imaging vitreous, Eye 16 (2002) 429–439.
[19] S.Y. Lin, K.H. Chen, W.T. Cheng, C.T. Ho, S.L. Wang, Preliminary identification of β-carotene in the vitreous asteroid bodies by micro-Raman spectroscopy and HPLC analysis, Microsc. Microanal. 13 (2007) 128–132.
[20] M. Neelam, N. Gorman, J. Nolan, O. O'Donovan, H.B. Wong, K.G.A. Eong, S. Beatty, Measurement of macular pigment: Raman spectroscopy versus Heterochromatic Flicker Photometry, Invest. Ophthalmol. Vis. Sci. 46 (2005) 1023–1032.
[21] P.S. Bernstein, M.D. Yoshida, N. Katz, R.W. McClane, W. Gellermann, Raman detection of macular carotenoid pigments in intact human retina, Invest. Ophthalmol. Vis. Sci. 39 (1998) 2003–2011.
[22] D.Y. Zhao, S.W. Wintch, I.V. Ermakov, W. Gellermann, P.S. Bernstein, Resonance Raman measurement of macular carotenoids in retinal, choroidal, and macular dystrophies, Arch. Ophthalmol. 12 (2003) 967–972.
[23] V.J. Glenn, J.R. Beattie, L. Barrett, N. Frizzell, S.R. Thorpe, M.E. Boulton, J.J. McGarvey, A.W. Stitt, Confocal Raman microscopy can quantify advanced glycation end product (AGE) modifications in Bruch's membrane leading to accurate, nondestructive prediction of ocular aging, FASEB J. 21 (2007) 3542–3552.
[24] K. Hosseini, F.H.M. Jongsma, F. Hendrikse, M. Motamedi, Non-invasive monitoring of commonly used intraocular drugs against endophthalmitis by Raman spectroscopy, Lasers Surg. Med. 32 (2003) 265–270.
[25] T.I. Sideroudi, N.M. Pharmakakis, G.N. Papatheodorou, G.A. Voyiatzis, Non-invasive detection of antibiotics and physiological substances in the aqueous humor by Raman spectroscopy, Lasers Surg. Med. 38 (2006) 695–703.
[26] M. Harz, P. Rösch, J. Popp, Vibrational spectroscopy – a powerful tool for the rapid identification of microbial cells at the single-cell level, Cytometry A 75A (2009) 104–113.
[27] P. Rosch, M. Harz, M. Schmitt, K.D. Peschke, O. Ronneberger, H. Burkhardt, H.W. Motzkus, M. Lankers, S. Hofer, H. Thiele, J. Popp, Chemotaxonomic identification of single bacteria by micro-Raman spectroscopy: application to clean-room-relevant biological contaminations, Appl. Environ. Microbiol. 71 (2005) 1626–1637.
[28] G.J. Puppels, H.S. Garritssen, G.M. Segers-Nolten, F.F. Mul, J. Greve, Raman microspectroscopic approach to the study of human granulocytes, Biophys. J. 60 (1991) 1046–1056.
[29] D.M. Mannie, T.J. McConnel, C. Xie, Y.Q. Li, Activation-dependent phases of T cells distinguished by use of optical tweezers and near-infrared Raman spectroscopy, J. Immunol. Methods 297 (2005) 53–60.
[30] E.L. Howes, P.W. Cole, V.K. Cruse, M. Pollycove, Quantitation of acute experimental ocular inflammation with 111 indium-leukocytes, Invest. Ophthalmol. Vis. Sci. 29 (1988) 4031–4038.
[31] M.D. De Smet, C.C. Chan, Regulation of ocular inflammation – what experimental and human studies have taught us, Prog. Retin. Eye Res. 20 (2001) 761–797.
[32] L. Silveira, S. Sathaiah, R.A. Zângaro, M.T.T. Pacheco, M.C. Chavantes, C.A.G. Pasqualucci, Correlation between near-infrared Raman spectroscopy and the histopathological analysis of atherosclerosis in human coronary arteries, Lasers Surg. Med. 30 (2002) 290–297.
[33] E.E. Rossi, L. Silveira, A.L.B. Pinheiro, S.R. Zamuner, F. Aimbire, M. Maia, M.T.T. Pacheco, Raman spectroscopy for differential diagnosis of endophthalmitis and uveitis in rabbit iris in vitro, Exp. Eye Res. 91 (2010) 362–368.
[34] A.R. Paula, L. Silveira, M.T. Pacheco, ProRaman: a program to classify Raman spectra, Analyst 134 (2009) 1203–1207.
[35] J.A. Alkrad, Y. Mrestani, D. Stroehl, S. Wartewig, R. Neubert, Characterization of enzymatically digested hyaluronic acid using NMR, Raman, IR, and UV/Vis spectroscopies, J. Pharm. Biomed. Anal. 31 (2003) 545–550.
[36] C.J. Lima, S. Sathaiah, L. Silveira, R.A. Zângaro, M.T.T. Pacheco, Development of catheters with low fiber background signals for Raman spectroscopic diagnosis applications, Artif. Organs 24 (2000) 231–234.
[37] D.F. Lopes, L. Silveira, M.N. Sibata, A.C. Carvalho, C. Pacheco-Soares, J. Saade, M.T.T. Pacheco, Use of dispersive Raman spectroscopy to detect the cytotoxic action of viscum album in adenocarcinoma of colon, J. Laser Appl. 21 (2010) 163–168.
[38] N. Stone, C. Kendall, J. Smith, P. Crow, H. Barr, Raman spectroscopy for identification of epithelial cancers, Faraday Discuss. 126 (2004) 141–157.
[39] R.A. Schachar, S.A. Solin, The microscopic protein structure of the lens with a theory for cataract formation as determined by Raman spectroscopy of intact bovine lenses, Invest. Ophthalmol. Vis. Sci. 14 (1975) 380–396.
[40] L.P. Choo-Smith, K. Maquelin, T. van Vreeswijk, H.A. Bruining, G.J. Puppels, N.A. Ngo Thi, C. Kirschner, D. Naumann, D. Ami, A.M. Villa, F. Orsini, S.M. Doglia, H. Lamfarraj, G.D. Sockalingum, M. Manfait, P. Allouch, H.P. Endtz, Investigating microbial (micro)colony heterogeneity by vibrational spectroscopy, Appl. Environ. Microbiol. 67 (2001) 1461–1469.
[41] E.L. Owes, Cellular and vascular responses in acute experimental ocular inflammation, Invest. Ophthalmol. Vis. Sci. 35 (1994) 4031–4038.
[42] S.J. Curnow, P.I. Murray, Inflammatory mediators of uveitis: cytokines e chemokines, Curr. Opin. Ophthalmol. 7 (2006) 532–537.